

pubs.acs.org/Macromolecules Article

Effects of Ionic Group Distribution on the Structure and Dynamics of Amorphous Polymer Melts

Supun S. Mohottalalage, Dipak Aryal, Bryce A. Thurston, Gary S. Grest,* and Dvora Perahia*



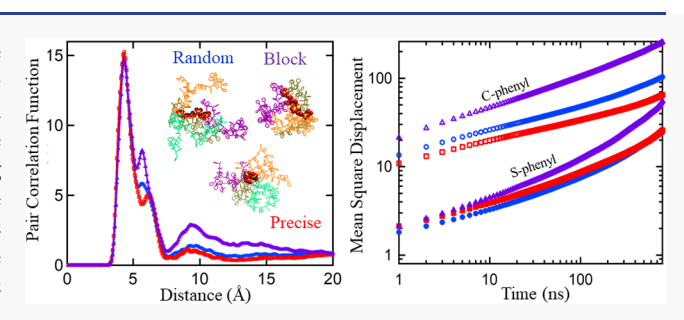
Cite This: Macromolecules 2022, 55, 217-223



ACCESS I

Metrics & More

ABSTRACT: Ionizable groups tethered to a polymer backbone often associate to form ionic clusters, whose features are determined by the balance of the polymer backbone and electrostatics. These assemblies impact the dynamics of the macromolecules and their ability to transport ions. Here, using fully atomistic molecular dynamics (MD) simulations, we investigate the effects of the distribution of ionizable groups along the polymer backbone on cluster characteristics and the resulting impacts on the structure and dynamics of amorphous polymers. Particularly, we probe polystyrene sulfonates (PSS) with



Article Recommendations

random, precise, and block configurations of the SO_3^- sulfonate groups along the backbone with Na^+ as the counterion. We find that the distribution of the ionic groups affects the shape and distribution of the clusters as well as the internal packing of the ionizable groups in the cluster and the number of unique chains that participate in each cluster, affecting the structure and the dynamics of the polymers. The signature of ionic clusters, observed in the static structure factor S(q) for all three distributions, is significantly more pronounced for the precise and blocky polymers compared to the random one. Remarkably, we find that the local mobility of the polymer segments is not only affected by the number and size of the clusters but also by the number of polymer chains associated with clusters.

INTRODUCTION

Polymers that consist of ionic groups tethered to their backbone often associate to form clusters that drive the structure and dynamics of these macromolecules. 1-3 They control the structure and dynamics of the polymers and impact the mechanical stability as well as ion and water transport characteristics in these materials, which in turn affect their many applications from clean energy to biotechnology. In the low ionic decoration regime, often termed the ionomer regime (less than ca. 20% decoration), both the electrostatic interactions and the chain conformation affect the properties of the polymers, where the distribution of ionic groups along the backbone affect both. However, the critical impact of the distribution of the ionic groups along the polymer backbone remains an open question predominantly since a vast number of studies have been constrained by synthetic routes that often produce a specific distribution. Here using molecular dynamics (MD) simulations, we investigate the effects of the distribution of ionizable groups along the polymer backbone on cluster formation and the interrelation with the structure and dynamics of amorphous polymers.

Driven by synthetic routes, a large number of experimental³⁻⁹ and computational¹⁰⁻¹⁴ studies have focused on polymers with random distribution of ionizable groups. These macromolecules cluster and constrain the dynamics of the chains as shown by Weiss et al.⁶ who showed that a small

fraction of ionizable groups on a short polystyrene, below the entanglement length, is sufficient to significantly slow the polymer motion. These clusters often dominate the structure of these melts and are characterized by an interaggregate distance signature (ionic peak) in the static scattering factor S(q), where q is the momentum transfer vector, measured by both small-angle X-ray scattering and neutron scattering. The shape of the aggregates is reflected in the line shape of the ionic peak and has been further probed by transmission electron microscopy, where within the resolution of the measurements, a significant number of ionic clusters appear spherical. ^{9,15} Further insight regarding chain conformation is obtained from the scaling of S(q) with q at the chain packing regime.

Recent synthetic efforts were able to tether ionizable groups at a precise distance through acyclic diene metathesis polycondensation, forming relatively short polymers with well-defined distribution of ionizable groups. ¹⁶ These polymers

Received: October 13, 2021 Revised: December 1, 2021 Published: December 23, 2021





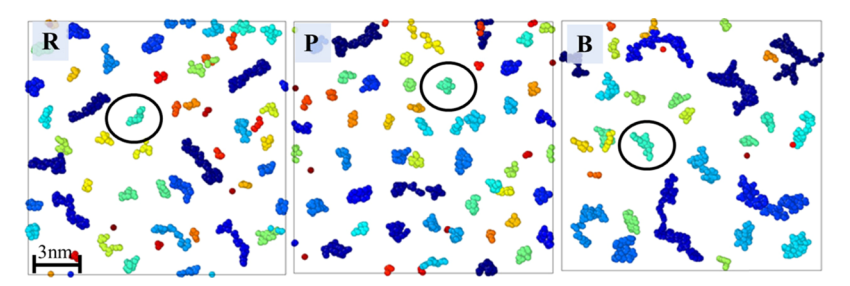


Figure 1. Visualization of SO_3^- groups in melts of random (R), precise (P), and block (B) PSS for f = 0.10 at 600 K after 1000 ns. Clusters in each system are colored based on the number of SO_3^- groups associated (red < orange < yellow < green < teal < blue). For clarity, 1/8 of the systems are shown. A black circled cluster represents the average cluster of SO_3^- groups for each system.

exhibit significant differences in their structure and dynamics in comparison with random copolymers, as have been shown by Seitz et al. for precisely sequenced poly(ethylene-co-acrylic acid) ionomers. The ionomer peak in these polymers exhibits a well-defined interaggregate correlation compared with randomly spaced materials, as has been shown by X-ray scattering and numerical simulations, with chain packing signatures that are typical to semicrystalline macromolecules.^{9,14} Computational studies were able to capture the higher intensity and narrower lines of the ionomer signature observed experimentally and provided further insight regarding the dynamics. Studies of the segmental motion by Frischknecht et al.¹⁷ on precise poly(ethylene-co-acrylic acid) ionomers showed that the local motion of the chains slows down as clusters are formed, which is in excellent agreement with quasielastic neutron scattering. Hall et al. 13 studied precise ionomer melts using coarse-grained models with explicit counterions and compared them with the corresponding random system. They observed that the clusters relax faster than the polymer for the precise ionomers; however, this is reversed for a random system. The behavior of the precise polymers is typical of semicrystalline polymers.

The structure and transport characteristics of polymers with random and precise distributions of ionizable groups along the polymer backbone are clearly distinctive. The fundamentals that under lie these differences, however, remain unresolved. Using atomistic MD simulations, the current study probes the effects of the distribution of the ionizable groups along the backbone of an amorphous model polymer on the shape and size of the ionic clusters along with the impact on the packing of the ionizable groups within the clusters. These are correlated with the mesoscopic structure and dynamics of the melts, providing insight into materials designed with desired structure-property characteristics. In particular, we investigate ionomer melts of random (R), precise (P), and block (B) polystyrene sulfonate (PSS) fully neutralized with Na+ counterions. The wealth of knowledge available for PSS is invaluable for focusing on the impact of distribution of the ionizable groups. Despite many ongoing uses of this polymer, the span of technologies is constantly expanding, where the interaction between clustering and properties is a key to their use. 18 Furthermore, PSS remains amorphous and therefore the results provide insight into the inherent effects of ionic group distribution. The correlations between the distribution of the ionizable groups along the polymer backbone, cluster characteristics, and adaptation ability of the material as resolved by MD simulations are discussed.

MODEL AND SIMULATION METHODS

Random, precise, and block PSS molecules of 80 monomers (molecular weight ~8950 g/mol) with 10% sulfonation were constructed using Polymer Builder and Amorphous Cell modules in BIOVIA Materials Studio. For the random system, eight sulfonated groups were randomly added to each chain. For the precise system, each chain had one sulfonation group every 10th monomer starting from the 5th monomer. Finally, for the block system, four sulfonated monomers were placed consecutively every 24th monomer resulting in polymers with two blocks of four sulfonated monomers per chain. These systems contained a total of 270, 248, and 280 molecules for random, precise, and block, respectively, with Na⁺ as the counterion.

The all-atom optimized potentials for liquid simulations (OPLS-AA) force field by Jorgensen et al. 19,20 were used to model the system. Additional parameters for the sulfonate groups are given in refs 21-23. The polymers were initially equilibrated using LAMMPS.²⁴ The intermolecular forces were described by Lennard-Jones interactions with attractive r^{-6} and repulsive r^{-12} terms and Coulomb interactions. The electrostatic interactions were calculated using particle-particle particle mesh with a real space cutoff of 1.2 nm and a precision of 10⁻⁶ for the attractive term of the Lennard-Jones interactions and 5×10^{-4} for the electrostatic interactions. The repulsive (r^{-12}) Lennard-Jones interaction is truncated at 1.2 nm. The reference system propagation algorithm²⁵ with a multi-time-scale integrator was used to accelerate the simulation. The time step is 1.0 fs for the bond, angle, dihedral, van der Waals interaction, and direct interaction part of the electrostatic interactions and 4.0 fs for longrange interactions. Periodic boundary conditions were used in all simulations. LAMMPS data files were converted into GRO-MACS²⁶⁻²⁸ [structure (.gro) and topology (.top)] because of enhanced efficiency and melts were further equilibrated. Conversion was carried out using a combination of ParmEd and InterMol tools.² The electrostatics was treated using the particle mesh Ewald³⁰ algorithm and a Fourier grid spacing of 0.12 nm. All harmonic bonds involving hydrogen atoms were replaced with constraints using the LINCS algorithm.³¹ The temperature was maintained using the Bussi-Parrinello thermostat (v-rescale)³² with a time constant of 0.1 ps. The system pressure was maintained at 1 bar using the barostat by Berendsen et al.³³ The simulations were carried out using a 2 fs time step. The MDAnalysis³⁴ toolkit was used to perform an equilibrium analysis.

All three melts were first equilibrated at 600 K at a constant pressure of 1 atm using the Nosé–Hoover thermostat and a barostat for \sim 5 ns in LAMMPS. The dielectric constant ε was then increased to 30 to reduce the residual electrostatic screening between the ionic groups. Increasing ε breaks the ionic clusters, allowing the chains to locally equilibrate. The melts were run for 30 ns at a constant volume after which the dielectric constant was reset to 1. Each of the systems was then run for 1000 ns in GROMACS at a constant volume at density $\rho = 0.94$ g/cm³. This procedure allowed us to follow the formation of the ionic clusters and dynamics of the chains. Ionic clusters were formed over a period of ca. 120–150 ns after ε was set to 1. After this period, no significant changes were observed in either

cluster sizes or their distribution. All results shown here are averaged over the last 850 ns of the run.

RESULTS

Illustrations of cluster morphologies of SO₃⁻ assemblies observed in random, precise, and block PSS melts are shown in Figure 1. Many of the ionic clusters for R-PSS are elongated, whereas the clusters are more globular in P-PSS melts with mixed structures of both elongated and globular for the B-PSS melts. The results for R-PSS are consistent with the elongated clusters observed by MD simulations in the study by Agrawal et al. Note that a rich variety of shapes have been observed for numerous ionomers; however, no clear driving forces for the different morphologies have been yet established.

The distribution of the ionizable groups along the backbone affects not only the topology of the clusters but also their size. The ionic cluster size distributions $N_{\rm nc}$, normalized to the total number of chains $N_{\rm n}$ are shown in Figure 2 as a function of $N_{\rm C}$,

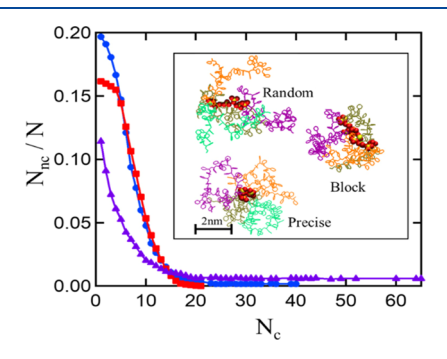


Figure 2. Number of clusters $N_{\rm nc}$, normalized to the total number of chains N, as a function of cluster size $N_{\rm c}$ (number of sulfur atoms), for random (blue circle), precise (red square), and block (purple triangle) PSS melts. The inset shows the snapshot of a cluster of ${\rm SO}_3^-$ groups (enlarged yellow and red spheres are sulfur and oxygen, respectively) and associated polymers chains for each system. For clarity, half the length of chains is shown. Different colors in the inset represent distinct chains.

the number of sulfur atoms per cluster. Two ionic groups are considered to be in the same cluster if two sulfur atoms are separated by a distance less than 6 Å, a number dictated by the chemical structure of the sulfonated groups. The average cluster sizes measured are 6.3, 5.8, and 10.1 for the random, precise, and block systems, respectively.

The cluster distributions are relatively broad for all three melts, the distribution of B-PSS being the broadest. The cluster distribution of the block chains exhibits a much longer tail, which shows that larger assemblies are formed.

The ionic clusters serve as physical cross-links in these ionomer melts and thus affect the structural stability of PSS melts compared to nonsulfonated PS. The ionic assembly may consist of ionizable groups tethered to different chains (distinct or unique chains) or groups that reside on the same backbone. The number of unique polymer chains $N_{\rm uc}$ associated with each of the clusters together with the size and shape of the clusters govern the overall dynamics of the melts. Illustrations of unique chains that contribute to an ionic cluster of an average size for each of the three systems are shown in the inset of Figure 2.

Ionic clusters of an average size consist of four unique chains for random and precise systems and three for the block system. The fraction of unique chains decreases with the increasing cluster size for all three systems as shown in Figure 3. At large N_{ct} , the number of unique chains is directly proportional to the

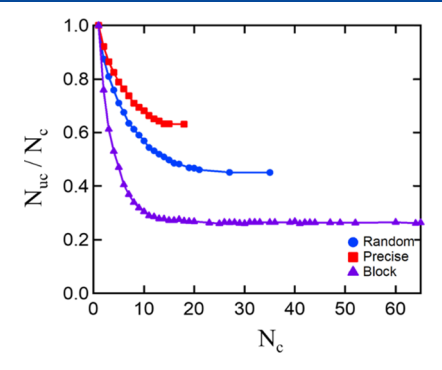


Figure 3. Averaged number of unique chains $N_{\rm uc}$ normalized to cluster size $N_{\rm c}$ for random, precise, and block PSS melts.

cluster size. Significantly fewer unique chains are associated with a given cluster size for the block melts compared to random and precise systems.

Further insight into the effects of the ionic distribution on the structure of the melts was obtained from the static structure factor $S(q) = |\sum_i b_i e^{iq \cdot r_i}|^2 / \sum_i b_i^2$, where q is the momentum transfer vector and b_i and r_i are the scattering length and position vectors of atom i, respectively. Due to the periodic boundary conditions, the wave vectors q are limited to $q = \frac{2\pi}{L} (n_{xv} n_{yv} n_z)$, where L is the length of the simulation cell and $n_{xv} n_{yv}$, and n_z are integers. S(q) was calculated using the scattering length of the elements for neutrons, which experimentally has provided an in-depth insight into the structure of amorphous polymers. The scattering lengths b_i for neutrons for each of the elements are listed in Table 1.

Table 1. Neutron Scattering Lengths of Elements³⁵

element	scattering lengths (10^{-15} m)
Н	-3.74
С	6.65
S	2.80
O	5.80
Na	3.63

S(q) as a function of q for the three different melts are shown in Figure 4a with the data averaged over the last 850 ns of the run. For high q, which corresponds to shorter intramolecular distances, the distribution of the ionic groups has hardly any effect. The correlation of the ionic clusters is

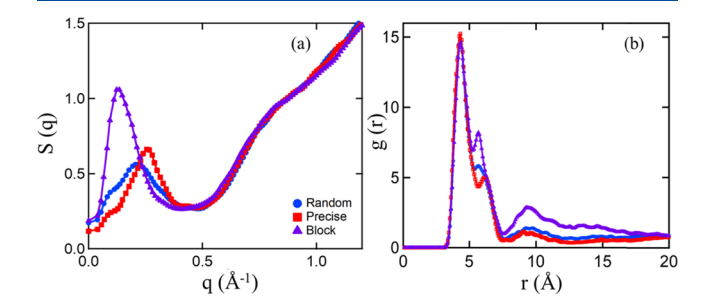


Figure 4. (a) S(q) as a function of q and (b) sulfur–sulfur radial distribution function for random, precise, and block PSS melts.

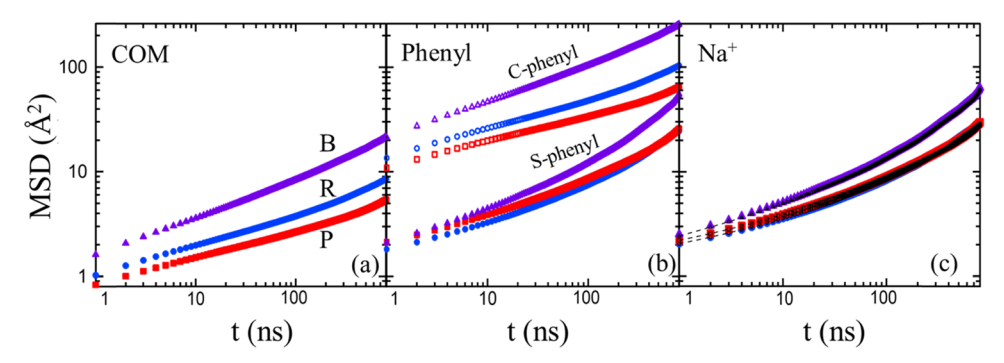


Figure 5. Mean square displacement as a function of time for (a) COM of chains, (b) phenyl rings without sulfonated groups (open symbols) and sulfonated phenyl rings (closed symbols), and (c) Na⁺ ions (closed symbol) and sulfur (black dash line and symbol) in the ionic group for the random (blue circle), precise (red square), and block (purple triangle) PSS melts.

expressed in a peak at low q centered around q = 0.214, 0.254, and 0.123 Å^{-1} , which corresponds to an average distance between ionic clusters of ~ 29 , 25, and 51 Å for random, precise, and block melts, respectively. While the precise and the blocky melts consist of rather similar interaggregate distances, the block copolymer is characterized by significantly larger dimensions. This low q peak is broader for the random polymer than for the precise and block melts indicating a relatively higher degree of interaggregate correlations even though the polymer is amorphous. Previous X-ray studies of precise polyethylene ionomers 9,16 have shown similar trends, though in this case the precise ionomers partially crystallize whereas the random polymer remains amorphous.

To characterize the internal correlations within the ionic clusters, we calculated the sulfur-sulfur (S-S) radial distribution function g(r). The results are shown in (b). For all three systems, the first peak at ~4.3 Å corresponds to the closest distance between two sulfur atoms in a cluster, whereas the second and third correlation peaks are notably different. The second correlation peak that captures the position of the next neighbor sulfur is rather broad for the random distribution melt and most sharp for the block copolymer. It is interesting to note that the molecular dimensions captured by g(r) and those of the ionic peak are entirely different. The trend of the second correlation peak in g(r) and the q dependence and intensity pattern of S(q) appear correlated. Higher correlations are more intense for the block copolymer melt, where significantly more sulfur atoms are tethered in proximity to each other. The pair correlation function shows clear differences in the packing of the sulfonated groups within the ionic clusters that appear to propagate to correlations in the nanometer dimensions reflected in S(q).

Following the observations of correlation between the packing of the sulfur atoms and the ionic peaks for different ionizable group distributions, we set to resolve the effects on dynamics. Measurements on two different length scales were carried out, the mean square displacement of the molecules and segmental dynamics. The overall mobility of the polymer chains was determined by measuring the mean square displacement, $MSD = \langle [r_i(t) - r_i(0)]^2 \rangle$ of the center of mass (COM) of the chains for the three systems as shown in Figure 5a. Even though the polymer does not move their own dimensions over the time of the simulations (1000 ns) due to the presence of the ionic groups, which act as physical crosslinks and are hence kinetically trapped, differences in the local segmental motion are observed between the three melts. For comparison, the mean squared radius of gyration is $\langle Rg^2 \rangle^{1/2} =$

4.8 nm for R-PSS, 5.9 nm P-PSS, and 4.0 nm for B-PSS. Interestingly, over the time scale of the measurement, the local mobility of the block chains is higher than those for the random and precise systems although the ionic clusters are larger. The distribution of ionic groups along the polymer chains affects the number of chains that participate in individual clusters as shown in Figure 3, altering the nature of the physical cross-links. For the blocky distribution, the connectivity of the polymer chains across clusters is lower compared to the two other distributions, while for precise and random distributions, the position of sulfonated phenyl rings along the polymer backbone reduces the local motion of the chains.

Zooming into the internal dynamics of the polymers, we compared the MSD of phenyl groups and sulfonated phenyl rings. As seen in Figure 5b, the motion of sulfonated phenyl rings for all distributions is significantly slower than that of the nonsulfonated rings, as previously observed for random PSS melts by Agrawal et al.¹¹ For random and precise melts, about 97.5% of the sulfonated groups reside within assemblies, thus they are more constrained, compared with the nonsulfonated rings. The motion of both sulfonated and nonsulfonated phenyl rings in the block melts is slightly faster compared to the motion in the random and precise melts in almost all of the sulfonated rings confined. In comparison with the local motion of both phenyl rings in the random and precise melt systems, we observe that in the precise melt system, the local motion of nonsulfonated rings is slower, whereas the motion of sulfonated rings is slightly higher than that in the random melt. MSD is averaged over all sulfonated groups in the melts; therefore, the number of confined S atoms and their internal packing within the clusters affect their motion. While hardly any S atoms reside outside the clusters, their MSD is directly correlated with the overall motion of the COM.

The relation between the dynamics of ionic species and the corresponding counterions is the critical factor that determines the transport ability of polymers. As seen in Figure 5c, the mobility of Na⁺ counterions in the block melt is slightly higher than those for the random and precise melts, showing similar trends of sulfonated phenyl rings as seen in Figure 5b. Furthermore, Figure 5c shows that Na⁺ ions are condensed on the ionic groups as they move largely with ionic groups in all three systems.

As segmental dynamics is key to understanding the mesoscopic motion of polymers, the normalized dynamic structure factor S(q,t)/S(q,0) was calculated. The dynamic structure factor $S(q,t)=\frac{1}{N}\sum_{i,j=1}^{N}b_ib_j\exp[iq.(r_i(t)-r_j(0))]$

captures correlated motion of different length scales, depending on q. S(q,t) was calculated using 300 configurations, each separated by 1 ns for the last 300 ns of the run. S(q,t) is calculated for q's on the order of magnitude of the interionic domain correlations and smaller length scales. Representative S(q,t) curves normalized to S(q,0) are shown in Figure 6 for two values of q.

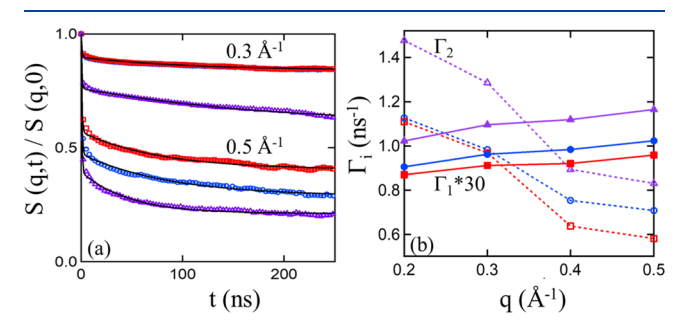


Figure 6. (a) S(q,t)/S(q,0) versus time t for the indicated q values (symbols) and double exponential fit (black solid line), (b) effective diffusion coefficient Γ_i as a function of q for the random (open circle), precise (open square), and block (open triangle) PSS melts. Slow (Γ_1) components are represented by solid symbols and lines and fast (Γ_2) components by open symbols and dashed lines.

For all q values measured over the entire time span, the relaxation is rather slow except at very early times, where a signature of very fast dynamics, compared to the polymer motion, is observed. At larger length scales, S(q,t) for the precise and random melts practically overlap where the dynamic scattering block melt decays slightly faster. With decreasing dimensions, away from the ionic peak, S(q,t) for the three melts decays slightly faster.

S(q,t) could not be captured by a single exponential pointing to complex dynamics. With chains being confined by the ionic clusters, a sum of two exponentials $S(q,t) = A_1 \mathrm{e}^{-\Gamma_1 t} + A_2 \mathrm{e}^{-\Gamma_2 t}$ was used to capture the behavior of S(q,t), where Γ_1 and Γ_2 are the effective diffusion coefficients with $\Gamma_1 < \Gamma_2$ and A_1 and A_2 ($A_1 + A_2 = 1$) are weight constants that provide the relative contributions of each of the dynamic processes to the overall dynamics. The fits are shown as a solid line in Figure 6a for all three PSS melts, and the corresponding effective diffusion coefficients are shown in Figure 6b. The values for slow and fast time constants and the corresponding pre-exponential factors are given in Table 2.

The slowest effective diffusion Γ_1 slightly increases with increasing q, in agreement with the S(q,t) previous results by Agrawal et al. for random melts. This is consistent with the ionic clusters acting as physical cross-linkers and inhibiting relaxation of the chains locally. A crossover region is observed for the faster relaxation time Γ_2 corresponding to a length scale of ~ 16 Å. This dimension is in the order of magnitude of the

Kuhn length of PS and attributed to the confinement region, where the chain dynamics are strongly affected by the chains being tethered to an ionic cluster. Both random and precise systems show almost similar magnitudes of dynamics and trends, with the block system exhibiting slightly faster dynamics compared to the random and precise systems.

CONCLUSIONS

Here, the structure and dynamics of PSS melts were studied as the distribution of ionizable groups along the polymer backbone was varied. The shape of the clusters and their size as well as internal packing of the sulfur groups within the clusters were determined and correlated with the structure as extracted by S(q) and dynamics as reflected in MSD and S(q,t). Though the effects observed appear small, particularly since the polymer is confined by the ionic clusters, the studies have provided new insight into the length scale of confinement and the correlation of cluster features and the macroscopic dynamics in such melts. We find that the distribution of sulfonated groups along the polymer chain backbone affects the shape, size, and packing of the ionizable groups within the cluster and in turn affects the mesoscopic properties. Random PSS melts consist of predominantly elongated clusters, whereas the clusters are more globular in precise PSS melts. A mix of both elongated and globular clusters coexist in block melts. The cluster size distribution for all melts is relatively broad, with the block melts comprised of larger clusters compared to random and precise melts. Furthermore, the internal packing of the sulfonated groups within the ionic clusters as reflected in the pair correlation function is affected by the distribution of the ionic groups along the polymer backbone, controlling the cohesion of the clusters. These differences in the packing of the sulfonated groups within the ionic clusters appear to propagate to correlations in the nanometer dimensions as reflected in S(q). As expected for all melts, the polymer motion is constrained on multiple length scales. However, fast and slow dynamic processes are detected by S(q,t) that are attributed directly to cluster-confined segments and those that reside further away.

The local mobility of the block chains is higher than the random and precise chains, even though the ionic clusters are larger. This brings to light an intriguing insight regarding the dynamics of the polymers, where the number of unique chains associated with one cluster is directly correlated with the dynamics of the polymers. Fewer unique chains associated with a given cluster size for the block melts compared to other systems result in faster dynamics. Finally, the Na⁺ ions are condensed on the ionic groups as they move largely with ionic groups in all three systems; however, counter dynamics in the block melt is slightly higher than the random and precise melts. The new insight into the correlations of ionizable group distributions along the amorphous polymer backbone provides

Table 2. Slow (Γ_1) and Fast (Γ_2) Effective Diffusion Coefficients and the Corresponding Pre-Exponential Factors Extracted from Double Exponential Fits for Random (R), Precise (P), and Block (B) PSS Melts

random				precise				block				
$q\ (\mathring{A}^{-1})$	$\Gamma_1 \; (ns^{-1})$	A_1	$\Gamma_2~(ns^{-1})$	A_2	$\Gamma_1 \ (ns^{-1})$	A_1	$\Gamma_2~(ns^{-1})$	A_2	$\Gamma_1 \ (ns^{-1})$	A_1	$\Gamma_2~(ns^{-1})$	A_2
0.2	0.030	0.10	1.13	0.89	0.029	0.10	1.11	0.91	0.034	0.19	1.48	0.81
0.3	0.032	0.12	0.98	0.88	0.030	0.12	0.97	0.88	0.036	0.24	1.29	0.76
0.4	0.033	0.29	0.75	0.71	0.031	0.34	0.64	0.65	0.037	0.27	0.89	0.73
0.5	0.034	0.37	0.71	0.63	0.032	0.43	0.58	0.57	0.039	0.32	0.83	0.67

an opening for the design of polymers whose clustering characteristics are controlled, affecting their potential applica-

AUTHOR INFORMATION

Corresponding Authors

Gary S. Grest — Sandia National Laboratories, Albuquerque, New Mexico 87185, United States; o orcid.org/0000-0002-5260-9788; Email: gsgrest@sandia.gov

Dvora Perahia — Department of Chemistry, Clemson University, Clemson, South Carolina 29634, United States; o orcid.org/0000-0002-8486-8645; Email: dperahi@g.clemson.edu

Authors

Supun S. Mohottalalage — Department of Chemistry, Clemson University, Clemson, South Carolina 29634, United States Dipak Aryal — Department of Chemistry, Clemson University, Clemson, South Carolina 29634, United States; Department of Chemical Engineering, University of Texas at Austin, Austin, Texas 78712, United States

Bryce A. Thurston – Sandia National Laboratories, Albuquerque, New Mexico 87185, United States

Complete contact information is available at: https://pubs.acs.org/10.1021/acs.macromol.1c02141

Notes

The authors declare no competing financial interest.

ACKNOWLEDGMENTS

D.P. gratefully acknowledges NSF Grant No. DMR-1611136 and DOE Grant No. DE-SC007908. The authors kindly acknowledge the use of computational resources provided by NSF MRI-1725573. This work was made possible in part by advanced computational resources deployed and maintained by Clemson Computing and Information Technology. This research used resources at the National Energy Research Scientific Computing Center (NERSC), a U.S. Department of Energy Office of Science User Facility operated under Contract No. DE-AC02-05CH11231. This work was performed, in part, at the Center for Integrated Nanotechnologies, a U.S. Department of Energy and Office of Basic Energy Sciences user facility. Sandia National Laboratories is a multimission laboratory managed and operated by the National Technology and Engineering Solutions of Sandia LLC, a wholly owned subsidiary of Honeywell International Inc., for the U.S. Department of Energy's National Nuclear Security Administration under Contract DE-NA0003525. The views expressed in this study do not necessarily represent the views of the U.S. DOE or the United States Government.

REFERENCES

- (1) Eisenberg, A.; Kim, J.-S., Introduction to ionomers; Wiley: New York, 1998.
- (2) Eisenberg, A. Clustering of ions in organic polymers. A theoretical approach. *Macromolecules* **1970**, *3*, 147–154.
- (3) Eisenberg, A.; Hird, B.; Moore, R. A new multiplet-cluster model for the morphology of random ionomers. *Macromolecules* **1990**, 23, 4098–4107.
- (4) Kirkmeyer, B. P.; Weiss, R. A.; Winey, K. I. Spherical and vesicular ionic aggregates in Zn-neutralized sulfonated polystyrene ionomers. *J. Polym. Sci., B: Polym. Phys.* **2001**, 39, 477–483.

- (5) Peiffer, D.; Weiss, R.; Lundberg, R. Microphase separation in sulfonated polystyrene ionomers. *J. Polym. Sci.: Polym. Phys. Ed.* **1982**, 20, 1503–1509.
- (6) Weiss, R.; Zhao, H. Rheological behavior of oligomeric ionomers. J. Rheol. 2009, 53, 191–213.
- (7) Zhou, N. C.; Chan, C. D.; Winey, K. I. Reconciling STEM and X-ray scattering data to determine the nanoscale ionic aggregate morphology in sulfonated polystyrene ionomers. *Macromolecules* **2008**, *41*, 6134–6140.
- (8) Moore, R. B.; Bittencourt, D.; Gauthier, M.; Williams, C. E.; Eisenberg, A. Small-angle X-ray scattering investigations of ionomers with variable-length side chains. *Macromolecules* **1991**, *24*, 1376–1382
- (9) Seitz, M. E.; Chan, C. D.; Opper, K. L.; Baughman, T. W.; Wagener, K. B.; Winey, K. I. Nanoscale morphology in precisely sequenced poly (ethylene-co-acrylic acid) zinc ionomers. *J. Am. Chem. Soc.* **2010**, *132*, 8165–8174.
- (10) Agrawal, A.; Perahia, D.; Grest, G. S. Cluster morphology-polymer dynamics correlations in sulfonated polystyrene melts: computational study. *Phys. Rev. Lett.* **2016**, *116*, No. 158001.
- (11) Agrawal, A.; Perahia, D.; Grest, G. S. Clustering effects in ionic polymers: Molecular dynamics simulations. *Phys. Rev. E: Stat., Nonlinear, Soft Matter Phys.* **2015**, 92, No. 022601.
- (12) Ma, B.; Nguyen, T. D.; Pryamitsyn, V. A.; Olvera de la Cruz, M. Ionic correlations in random ionomers. *ACS Nano* **2018**, *12*, 2311–2318.
- (13) Hall, L. M.; Stevens, M. J.; Frischknecht, A. L. Dynamics of model ionomer melts of various architectures. *Macromolecules* **2012**, 45, 8097–8108.
- (14) Hall, L. M.; Seitz, M. E.; Winey, K. I.; Opper, K. L.; Wagener, K. B.; Stevens, M. J.; Frischknecht, A. L. Ionic aggregate structure in ionomer melts: effect of molecular architecture on aggregates and the ionomer peak. *J. Am. Chem. Soc.* **2012**, *134*, 574–587.
- (15) Register, R. A. Morphology and structure—property relationships in random ionomers: Two foundational articles from Macromolecules. *Macromolecules* **2020**, *53*, 1523–1526.
- (16) Baughman, T. W.; Chan, C. D.; Winey, K. I.; Wagener, K. B. Synthesis and morphology of well-defined poly (ethylene-co-acrylic acid) copolymers. *Macromolecules* **2007**, *40*, 6564–6571.
- (17) Frischknecht, A. L.; Paren, B. A.; Middleton, L. R.; Koski, J. P.; Tarver, J. D.; Tyagi, M.; Soles, C. L.; Winey, K. I. Chain and ion dynamics in precise polyethylene ionomers. *Macromolecules* **2019**, *52*, 7939–7950.
- (18) Labriola, L.; Jadoul, M. Sodium polystyrene sulfonate: still news after 60 years on the market. *Nephrol., Dial., Transplant.* **2020**, 35, 1455–1458.
- (19) Jorgensen, W. L.; Maxwell, D. S.; Tirado-Rives, J. Development and testing of the OPLS all-atom force field on conformational energetics and properties of organic liquids. *J. Am. Chem. Soc.* **1996**, 118, 11225–11236.
- (20) Jorgensen, W. L.; Madura, J. D.; Swenson, C. J. Optimized intermolecular potential functions for liquid hydrocarbons. *J. Am. Chem. Soc.* **1984**, *106*, 6638–6646.
- (21) He, X.; Guvench, O.; MacKerell, A. D., Jr.; Klein, M. L. Atomistic simulation study of linear alkylbenzene sulfonates at the water/air interface. *J. Phys. Chem. B* **2010**, *114*, 9787–9794.
- (22) Cannon, W. R.; Pettitt, B. M.; McCammon, J. A. Sulfate anion in water: model structural, thermodynamic, and dynamic properties. *J. Phys. Chem.* **1994**, *98*, 6225–6230.
- (23) Chandrasekhar, J.; Spellmeyer, D. C.; Jorgensen, W. L. Energy component analysis for dilute aqueous solutions of lithium (1+), sodium (1+), fluoride (1-), and chloride (1-) ions. *J. Am. Chem. Soc.* **1984**, *106*, 903–910.
- (24) Plimpton, S. Fast parallel algorithms for short-range molecular dynamics. *J. Comput. Phys.* **1995**, *117*, 1–19.
- (25) Tuckerman, M.; Berne, B. J.; Martyna, G. J. Reversible multiple time scale molecular dynamics. *J. Chem. Phys.* **1992**, *97*, 1990–2001.
- (26) Pronk, S.; Páll, S.; Schulz, R.; Larsson, P.; Bjelkmar, P.; Apostolov, R.; Shirts, M. R.; Smith, J. C.; Kasson, P. M.; Van Der

- Spoel, D. GROMACS 4.5: a high-throughput and highly parallel open source molecular simulation toolkit. *Bioinformatics* **2013**, *29*, 845–854.
- (27) Abraham, M. J.; Murtola, T.; Schulz, R.; Páll, S.; Smith, J. C.; Hess, B.; Lindahl, E. GROMACS: High performance molecular simulations through multi-level parallelism from laptops to supercomputers. *SoftwareX* **2015**, *1*, 19–25.
- (28) Berendsen, H. J.; van der Spoel, D.; van Drunen, R. GROMACS: a message-passing parallel molecular dynamics implementation. *Comput. Phys. Commun.* **1995**, *91*, 43–56.
- (29) Shirts, M. R.; Klein, C.; Swails, J. M.; Yin, J.; Gilson, M. K.; Mobley, D. L.; Case, D. A.; Zhong, E. D. Lessons learned from comparing molecular dynamics engines on the SAMPL5 dataset. *J. Comput.-Aided Mol. Des.* **2017**, *31*, 147–161.
- (30) Essmann, U.; Perera, L.; Berkowitz, M. L.; Darden, T.; Lee, H.; Pedersen, L. G. A smooth particle mesh Ewald method. *J. Chem. Phys.* 1995, 103, 8577–8593.
- (31) Hess, B.; Bekker, H.; Berendsen, H. J.; Fraaije, J. G. LINCS: a linear constraint solver for molecular simulations. *J. Comput. Chem.* 1997, 18, 1463–1472.
- (32) Bussi, G.; Donadio, D.; Parrinello, M. Canonical sampling through velocity rescaling. *J. Chem. Phys.* **2007**, *126*, No. 014101.
- (33) Berendsen, H. J.; Postma, J. V.; van Gunsteren, W. F.; Dinola, A.; Haak, J. R. Molecular dynamics with coupling to an external bath. *J. Chem. Phys.* **1984**, *81*, 3684–3690.
- (34) Michaud-Agrawal, N.; Denning, E. J.; Woolf, T. B.; Beckstein, O. MDAnalysis: a toolkit for the analysis of molecular dynamics simulations. *J. Comput. Chem.* **2011**, 32, 2319–2327.
- (35) Sears, V. F. Neutron scattering lengths and cross sections. *Neutron News* **1992**, *3*, 26–37.
- (36) Kanaya, T.; Kaji, K.; Kitamaru, R.; Higgins, J. S.; Farago, B. Dynamics of polyelectrolyte solutions by neutron spin echo: molecular weight dependence. *Macromolecules* **1989**, *22*, 1356–1359.
- (37) Nyström, B.; Roots, J.; Higgins, J.; Gabrys, B.; Peiffer, D.; Mezei, F.; Sarkissian, B. Dynamics of polystyrene sulfonate ionomers in solution. A neutron spin-echo study. *J. Polym. Sci., Part C: Polym. Lett.* 1986, 24, 273–281.

□ Recommended by ACS

Conformation of a Comb-like Chain in Solution: Effect of Backbone Rigidity

Xinghong Mai, Mingming Ding, et al.

MARCH 17, 2023

ACS OMEGA

READ 🗹

Addressing Nanocomposite Systems via 3D-SCFT: Assessment of Smearing Approximation and Irregular Grafting Distributions

Constantinos J. Revelas, Doros N. Theodorou, et al.

FEBRUARY 13, 2023

MACROMOLECULES

READ 🗹

Response of Sulfonated Polystyrene Melts to Nonlinear Elongation Flows

Supun S. Mohottalalage, Dvora Perahia, et al.

JANUARY 27, 2023

MACROMOLECULES

READ 🗹

Chain Confinement and Anomalous Diffusion in the Cross over Regime between Rouse and Reptation

Aakash Sharma, Dieter Richter, et al.

NOVEMBER 21, 2022

ACS MACRO LETTERS

READ 🗹

Get More Suggestions >